Molecular dynamics simulation for chemically reactive substances. Fluorine

Frank H. Stillinger and Thomas A. Weber
AT&T Bell Laboratories, Murray Hill, New Jersey 07974

(Received 28 December 1987; accepted 5 January 1988)

Molecular dynamics computer simulation has been utilized to study physical and chemical properties of the highly reactive element fluorine in its fluid phases. The underlying model approximates the energy of the ground electronic state for an arbitrary collection of fluorine atoms with a combination of two and three atom interactions. The classical simulation employed 1000 atoms subject to periodic boundary conditions. Diatomic molecules spontaneously form and are stable at low temperatures, but dissociation and atom exchange reactions occur at high temperatures. Steepest-descent quenching on the potential energy hypersurface reveals the presence of a temperature-independent inherent structure for the low-temperature undissociated liquid. Dissociation is found to be strongly enhanced at high density owing to relatively strong solvation by diatomics of chemically unbonded fluorine atoms. Slow cooling of the fluid from well above the critical temperature, at one-eighth of the triple-point density, produced a condensation phenomenon driven by the weak van der Waals attractions that operate between intact diatomic molecules.

I. INTRODUCTION

Computer simulation studies, both the Monte Carlo and molecular dynamics variants, have generated important insights into the nature of strongly interacting many-body systems. However, most of the substances thus far studied have been chemically inert, as in the case of liquified noble gases.[1,2] Recently, a few examples have been reported in which chemical reactivity was examined, i.e., the simulations involved explicit descriptions of chemical bond formation and disruption.[3–6] This seems to open the way for simulation of a wide range of important chemical processes in solid, liquid, and gas phases, as well as at interfaces.

For nonreactive substances it often suffices to represent interactions by additive pair potentials for the constituent particles. But when directional and saturating chemical bonds can form between those particles the pairwise additivity assumption fails. In some cases it seems that combinations of two-body and three-body potentials suffice to represent the main features of chemical binding. The tetravalent semiconductor silicon[7–9] and the divalent chalcogenide sulfur[10,11] have been represented this way and simulated via the molecular dynamics method.

The present paper reports an extension of this approach to the monovalent element fluorine. We view the present project as a necessary precursor to simulation modeling of fluorine reactions with other substances, such as the etching of metal or semiconductor crystals.

The details of our fluorine potential are presented and explained in the following Sec. II. The balance between two-atom and three-atom interactions has been delicately arranged to give proper stable diatomics that engage in weak van der Waals attractions, while permitting realistic exchange reactions to occur at sufficiently high excitation.

At low temperatures the model yields exclusively intact diatomic molecules, and Sec. III contains results for the pair correlation function in the liquid phase formed by those diatomics.

If the temperature is sufficiently high it becomes feasible for the F_2 molecules to undergo spontaneous dissociation into atoms. The molecular dynamics simulation technique then offers a tool for the study of chemical reaction rates and of the association–dissociation equilibrium constant. Section IV exhibits some results obtained for temperature dependence of the degree of dissociation. Such results have been obtained both at the triple-point density, and at one-eighth of that density (corresponding to a moderately compressed gas). Solvation is sufficiently strong for the F atoms produced by dissociation to cause the degree of dissocation at constant temperature to increase with density, in violation of the usual conclusion of Le Chatelier's principle.

Section V presents a study of the vapor condensation to form the liquid.

Several additional points and conclusions are offered in Sec. VI.

It should be mentioned that liquid fluorine (and the other liquid halogens chlorine and bromine) have been previously simulated with the molecular dynamics approach by Singer, Taylor, and Singer.[12] However, the model utilized consisted of "rigid dumbbells" and therefore differed from the present case in that intramolecular vibration and the possibility of exchange and dissociation reactions were absent. We comment on this prior work at the appropriate place below.

II. INTERACTION POTENTIAL

Computer simulation studies must be based on an acceptable approximation to the ground electronic state potential surface Φ for the collection of atoms involved. Consistent with our earlier modeling for reactive substances[7,10,11] we assume that Φ can be approximated by a linear combination of two-atom and three-atom interactions

$$\Phi(\mathbf{r}_1 \cdots \mathbf{r}_N) \cong \sum_{i<j} v_2(r_{ij}) + \sum_{i<j<k} v_3(\mathbf{r}_i,\mathbf{r}_j,\mathbf{r}_k) . \quad (2.1)$$

The component functions v_2 and v_3 need to be chosen to satisfy both physical accuracy as well as computational fea-

 0021-9606/88/085123-11$02.10

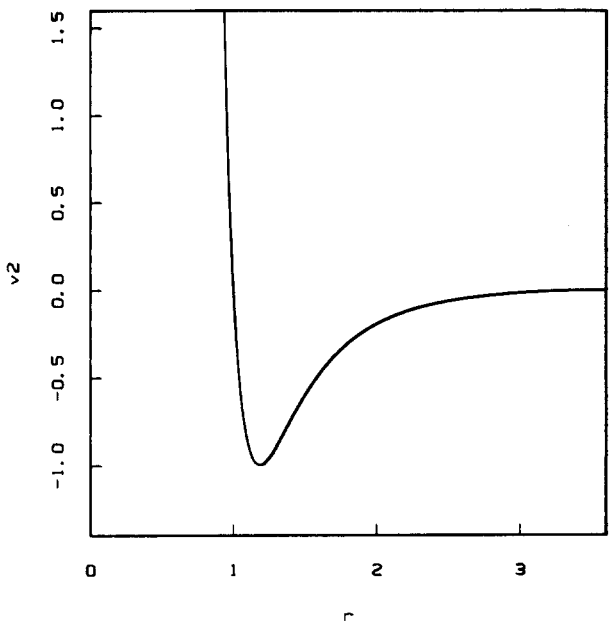

FIG. 1. Pair potential v_2 for the fluorine model. This function vanishes identically for $r \geqslant 3.6$.

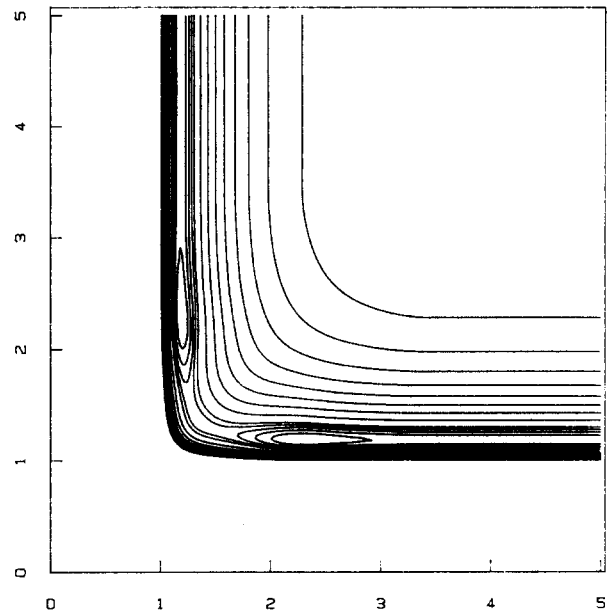

FIG. 2. Potential energy contours for the linear arrangement of three fluorine atoms. In reduced energy units the specific contours shown correspond to -1.01, -0.98, -0.95, -0.92, -0.89, and -0.8 to -0.1 in steps of 0.1.

sibility when large numbers of atoms are involved.

We have selected the pair potential v_2 to give a good representation of the isolated diatomic molecule F_2. Using reduced units for convenience (energy unit $\epsilon = 38.295$ kcal/mol $= 1.66$ eV; length unit $\sigma = 1.2141$ Å) the specific form used is

$$v_2(r) = A(r^{-8} - r^{-4})\exp[(r-3.6)^{-1}] \quad (0<r<3.6),$$
$$= 0 \quad (3.6 \leqslant r)\,. \tag{2.2}$$

The multiplier A causes v_2 to have a minimum of depth -1:

$$A = 6.052\,463\,017\,. \tag{2.3}$$

Figure 1 displays the reduced pair potential.

By construction v_2 produces the correct bond length (1.435 Å[13]) for the F_2 molecule; in reduced units the potential minimum occurs at

$$r_e = 1.181\,99\,. \tag{2.4}$$

In the same reduced units

$$v_2''(r_e) = 24.96\,, \tag{2.5}$$

and the corresponding harmonic vibration frequency for a pair of bonded F^{19} atoms is 896.9 cm^{-1} (892 cm^{-1}, experimental[13]). The pair potential depth has been chosen to be consistent with the measured spectroscopic constant D_0° for F_2.[14]

The major role of v_3 is to prevent formation of more than one covalent bond to each fluorine atom. If a third fluorine atom were to approach an already-formed F_2 molecule from any direction, the resulting v_3 must be sufficiently large and positive (at least in the distance range comparable to covalent bond length) to outweigh the attractions inherent in the two new v_2 terms that arise. If this is the case the most stable arrangements of a large collection of fluorine atoms will automatically consist of collections of diatomics. We also demand that the combination of two-atom and three-atom potentials produces weak van der Waals attractions between neighboring diatomic molecules.

Providing a reasonable account of the three-atom exchange process

$$F + F_2 \rightleftarrows F_2 + F \tag{2.6}$$

is an important further requirement and a stringent limitation on possible v_3 functions. Unfortunately, there does not seem to be yet either an experimental or a theoretical determination of this three-body potential surface. Therefore, we have assumed tentatively that the well-determined $H + H_2$ surface[15] could approximately be scaled (in distance and energy) to the case of fluorine. This implies that the transition state for the exchange process (2.6) occurs in a linear symmetrical arrangement of the three atoms, with an energy lying above that of widely separated atom plus diatomic (but by an amount less than ten percent of the diatomic's covalent bond strength).

We have used the following representation for v_3:

$$v_3(\mathbf{r}_1,\mathbf{r}_2,\mathbf{r}_3) = h(r_{12},r_{13},\theta_1) + h(r_{21},r_{23},\theta_2) + h(r_{31},r_{32},\theta_3)\,, \tag{2.7}$$

where h is symmetric in its first two variables, and where θ_i is the angle subtended at atom i by the other two atoms. In reduced units as before,

$$h(r,s,\theta) = 8.4(rs)^{-4}\exp[(r-3.6)^{-1} + (s-3.6)^{-1}] + (50 - 25\cos^2\theta)\exp[3(r-2.8)^{-1} + 3(s-2.8)^{-1}] \tag{2.8}$$

provided $0 < r,s < 2.8$; the last term disappears if either r or s exceeds 2.8; and h vanishes identically if either r or s exceeds 3.6.

Figure 2 shows a contour plot for the potential energy of the linear arrangement of three fluorine atoms. As required the transition state is attained in the symmetrical configuration, with bonds stretched from r_e to

$$r^{\ddagger} = 1.293 . \tag{2.9}$$

The potential energy of this configuration is found to be

$$\Phi^{\ddagger} = -0.9352 \tag{2.10}$$

or 0.0648 (equivalently 2.48 kcal/mol) above the separated $F + F_2$ value.

Figure 2 clearly shows a pair of potential minima flanking the transition state. These correspond to the odd fluorine atom weakly solvated by the diatomic in the linear structure. The three-atom potential energy at these minima is approximately -1.040. However, they do not correspond to the global minimum for three fluorine atoms, which instead has the shape of an isosceles triangle (sides 1.194, 2.386, 2.386) and potential energy -1.071.

A full search of the four-atom configuration space reveals as required that the global minimum corresponds to a pair of weakly attracting diatomic molecules. The arrangement consists of an elongated tetrahedron. The two F_2 molecules are equivalent and mutually perpendicular with covalent bond lengths 1.198, slightly elongated compared to the equilibrium distance r_e for an isolated diatomic. The four nonbonded distances are 2.54, and the potential energy of the cluster is $-2.010\,27$.

We remark in passing that the generic LEPS form for atomic interaction surfaces is often used to study exchange reactions.[16] As it is usually applied, however, this form does not produce van der Waals attractions such as those underlying the solvation minima in Fig. 2. Since much of our own interest lies in the study of condensed phase properties, we have taken the position that such attractions were a necessary attribute of any potential function to be used in computer simulation.

In a companion study[17] Hankinson and Weber have examined gas-phase structures and reaction dynamics for several fluorine clusters, using the present Φ prescription. They find a particularly illuminating structure giving the lowest energy for seven F_2 molecules. It is shown in Fig. 3. A central F_2 is hexagonally surrounded by six neighboring F_2's. These latter display a slight helical twist around the central core, rendering the cluster optically active. This structure appears to be closely related to the crystal structure of α fluorine, which consists of nearly close-packed hexagonal layers of molecules, where each molecule has its axis tipped $\pm 18°$ from the normal to the plane of those layers.[18]

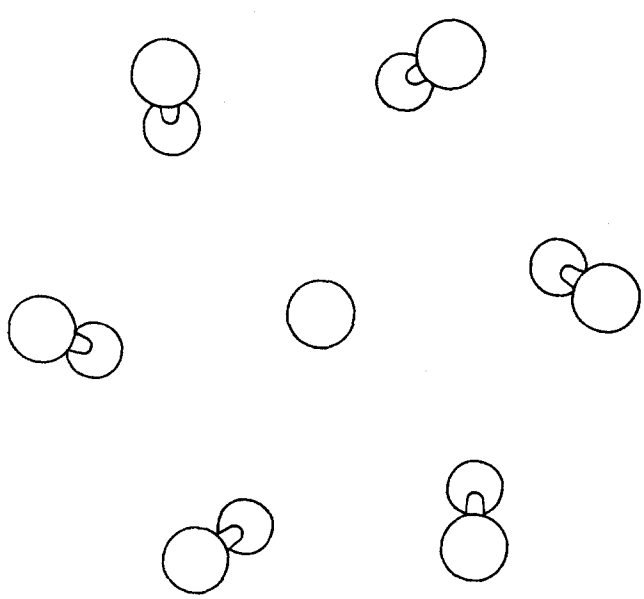

FIG. 3. Sixfold symmetric cluster found by Hankinson and Weber (Ref. 17) to be one of the structures giving the global potential energy minimum for 14 fluorine atoms.

III. LIQUID STRUCTURE

Molecular dynamics has been used to investigate the short-range order in liquid fluorine, employing the approximate potential function Φ explained in the preceding Sec. II. Although the presence of three-atom interactions slows the program execution substantially compared to more traditional simulation work in which they are absent, we have been able to examine systems of 1000 fluorine atoms. This system size should suffice to represent bulk liquid.

The experimental melting point of molecular fluorine is 53.54 K, and the mass density of the liquid at this temperature and ambient pressure is 1.713 g/cm^3.[19] The corresponding values in reduced units are

$$T_m^* = 0.002\,779 ,$$
$$\rho^* = 0.097\,173 . \tag{3.1}$$

The liquid density is achieved by placing the 1000 atoms in a cubical cell (with periodic boundary conditions) having reduced edge length 21.7513.

In order to initiate the molecular dynamics simulation for the cold liquid, the atoms were placed in the periodic cell in a regular arrangement consisting of intact parallel diatomic molecules, with small random velocities for each atom. In order to assure that these molecules remain bonded (as they should) in this low-temperature regime, the starting density was purposely taken anomalously low,

$$\rho^*(\text{initial}) = 0.064 , \tag{3.2}$$

by expanding the cubical cell appropriately. As the first few molecular dynamics sequences were carried out ρ^* was increased in stages until the value in Eq. (3.1) was attained.

The natural time unit for the classical dynamics is

$$\tau = \sigma(m/\epsilon)^{1/2} = 4.1817 \times 10^{-14}\ \text{s} . \tag{3.3}$$

We have used the standard fifth-order Gear algorithm[20] to integrate the Newtonian equations of motion for the 1000 fluorine atoms, with time increments 0.02τ (at low temperature) or 0.01τ (at the higher temperatures investigated). After appropriate equilibration runs at any temperature and density of interest, statistical averages were typically accumulated over runs consisting of 1000 or 2000 time steps.

Our primary interest in the low-temperature liquid concerns its short-range molecular order. The conventional device for viewing and interpreting this order is the atom–atom pair correlation function $g(r,T,\rho)$. We have evaluated this function for the fluorine model over a wide range of temperature. Figure 4 shows the pair correlation function evaluated for the liquid at reduced temperature 0.002 77, essentially at the experimental triple point. The sharp and isolated first peak around reduced distance 1.25 represents the chemically bonded pairs, and its area reflects the fact that exactly 500

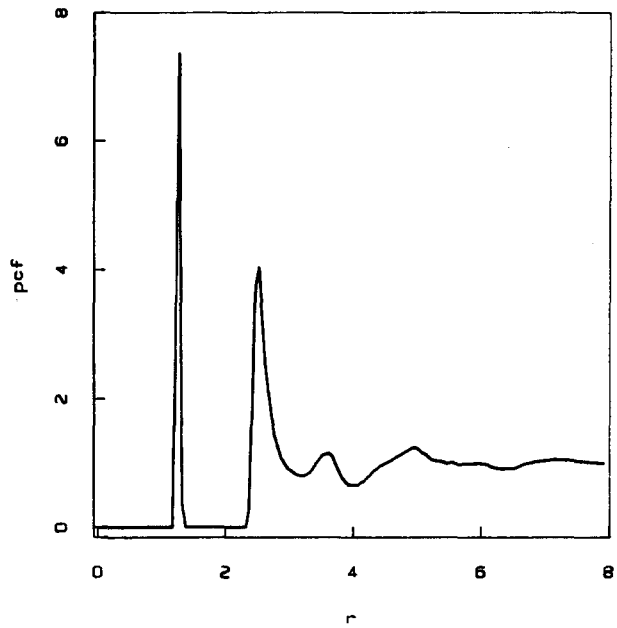

FIG. 4. Pair correlation function for the liquid at $T^* = 0.002\,77$, $\rho^* = 0.097\,173$, the experimental triple point.

bonds are present during the entire run at this temperature. Subsequent peaks beyond reduced distance 2 reveal the presence of intermolecular short-range order, i.e., arrangement preferences for neighboring diatomics. This short-range order has died away ($g \approx 1$) when r increases to about 8.

The effect of increasing temperature emerges from comparing Fig. 4 with Fig. 5. The latter presents the pair correlation function evaluated at reduced temperature 0.0165 (319 K), but with the liquid confined to the same triple-point density. The covalent bond peak is still isolated but has become lower and broader due to increased vibrational amplitudes; nevertheless its area still represents exactly 500 intact chemical bonds. Larger-distance intermolecular features are more or less present at the same locations as before but rendered less distinct by the more vigorous thermal motions.

We have also examined many temperatures between the extremes of Figs. 4 and 5. The corresponding pair correlation functions as expected smoothly interpolate between the functions shown.

Interpretation of short-range order in simulated liquids can often be facilitated by means of steepest-descent mapping on the potential energy hypersurface to local minima.[21–25] This can be carried out, in principle, for any representative collection of configurations selected from the equilibrium state of interest. Such mapping removes the obscuring influence of thermal vibrations away from the mechanically stable packings (potential minima) and consequently produces substantial "image enhancement" for the short-range order. In the wide variety of simulated liquids that have been examined with this steepest descent tool, one discovers a virtually temperature-independent inherent structure underlying the stable liquid phase. Temperature changes in molecular distribution functions such as that illustrated by Figs. 4 and 5 result almost exclusively from thermally-excited excursions away from potential minima.[26] A clear motivation exists for applying the steepest-descent mapping to the present fluorine model to see if a temperature-independent inherent structure also exists for this diatomic liquid.

Carrying out steepest-descent mapping for a 1000-atom system with nonadditive interactions is a very demanding numerical task. Consequently we have been limited to one such mapping for each of a small number of molecular dynamics runs. The few results obtained necessarily bear significant statistical uncertainty, but we believe they still have substantial interpretive value.

Figures 6 and 7, respectively, present the "quenched

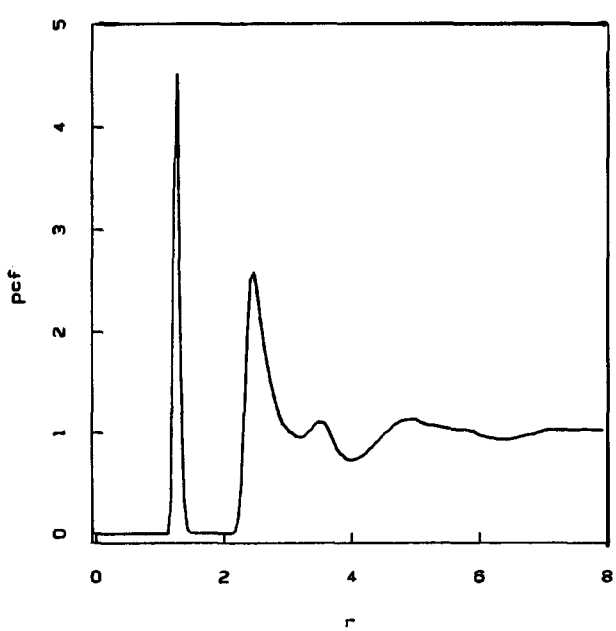

FIG. 5. Pair correlation function for the hot liquid at $T^* = 0.0165$, $\rho^* = 0.097\,173$.

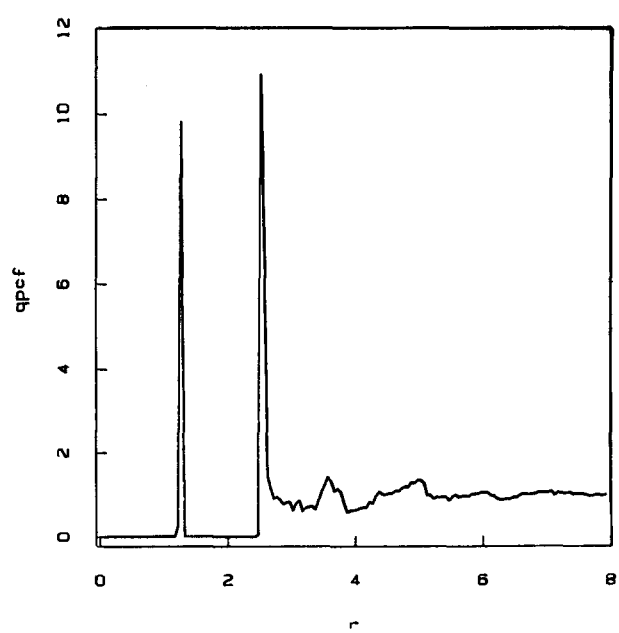

FIG. 6. Quenched pair correlation function obtained by steepest-descent mapping from the final configuration of the triple-point state represented in Fig. 4 ($T^* = 0.002\,77$, $\rho^* = 0.097\,173$).

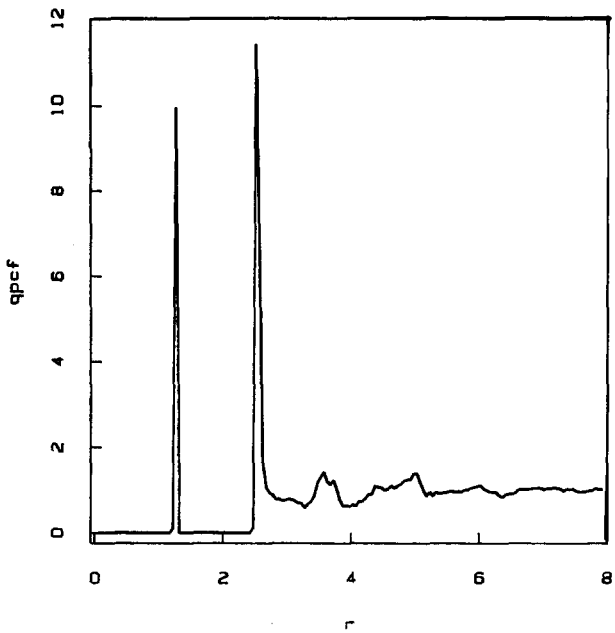

FIG. 7. Quenched pair correlation function obtained by steepest-descent mapping from the final configuration of the hot liquid state represented in Fig. 5.

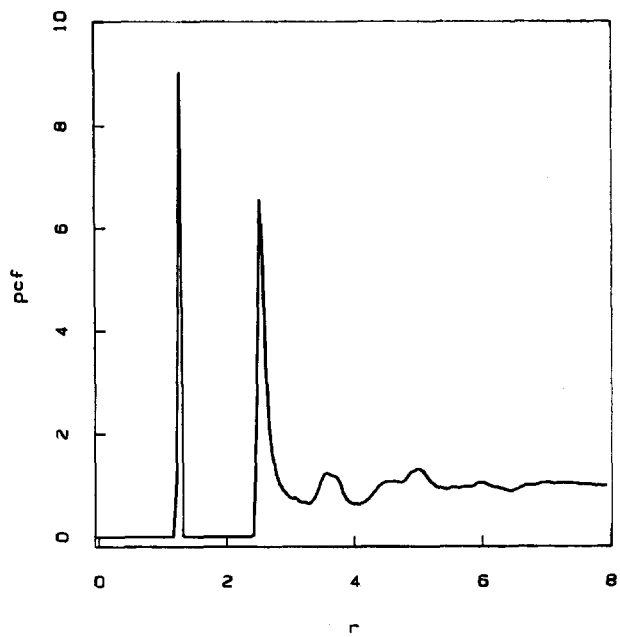

FIG. 8. Pair correlation function for a deeply supercooled noncrystalline state at $T^* = 4.96\times10^{-4}$, $\rho^* = 0.097\,173$.

pair correlation functions" obtained from the thermodynamic states represented earlier in Figs. 4 and 5. Specifically these are the pair correlation functions evaluated for the system, each at a single potential energy minimum that was obtained by subjecting the final configuration of the corresponding molecular dynamics run to the steepest-descent mapping.

The most striking feature presented by the results in Figs. 6 and 7 is the extreme narrowing of the first intermolecular peak (located in both cases at $r = 2.53$). Subsequent intermolecular features at larger r have experienced much more modest enhancements. The intramolecular peak has narrowed somewhat, but still retains a natural width due to static stresses frozen into the amorphous packings of fluorine molecules.

Within the prevailing statistical uncertainty the quench pair correlation functions in Figs. 6 and 7 appear to be the same, and to convey therefore an inherent structure for the model liquid fluorine. From the area under the sharp intermolecular peak we conclude that in this inherent structure an average of about eight nonbonded atoms are arranged on a spherical shell around any given atom.

In the case of good glass-forming liquids (which evidently fluorine is not, experimentally) slow cooling below the melting point and into the deeply supercooled regime should encourage the system to enter anomalously low-potential-energy amorphous regions of configuration space. To see if such behavior was implicit in our fluorine model, a series of molecular dynamics runs were carried out during which the 500-molecule system was cooled in stages, without crystallization, to reduced temperature 4.96×10^{-4} (9.6 K). Figures 8 and 9, respectively, show the correlation function, and the final-configuration quenched correlation function from steepest-descent mapping, for this metastable state. Within the given error limits, the quenched pair correlation function is the same as those derived from the higher temperature states. Table I gives energies of the mechanically stable packings for Figs. 6, 7, and 9 (as well as a few other states to be discussed below), and shows that the last of these three is not significantly lower than the other two. It seems that the temperature-independent inherent structure hypothesis extends into the strongly supercooled liquid regime for the present fluorine model.

Singer, Taylor, and Singer have used the molecular dynamics technique to simulate the liquid halogens.[12] Their model uses rigid diatomics (fixed bond lengths) with each

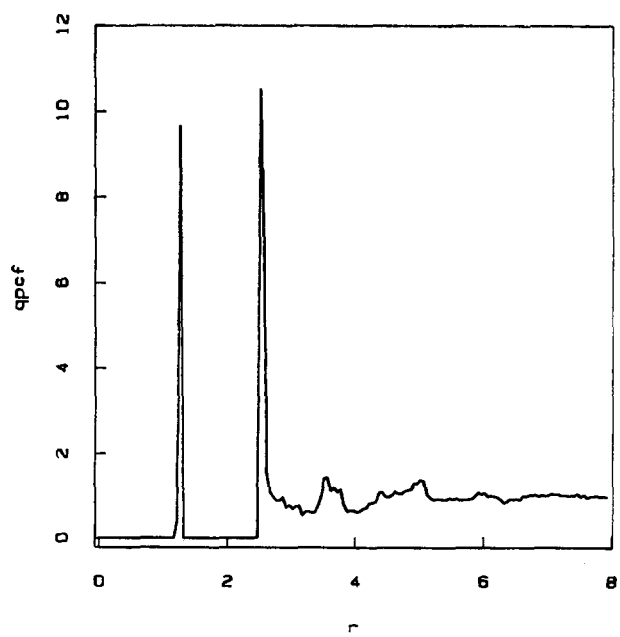

FIG. 9. Quenched pair correlation function obtained by steepest-descent mapping from the final configuration of the deeply supercooled state represented in Fig. 8 ($T^* = 4.96\times10^{-4}$, $\rho^* = 0.097\,173$).

TABLE I. Quench energies (potential energy minima) obtained by steepest-descent mapping from final configurations in various thermodynamic states.

ρ^*	Initial T^*	$\langle\Phi\rangle^a$	$\Phi_q{}^b$
0.012 147	0.079 6	− 450.176 38	− 486.580 045 730
0.012 147	0.124	− 409.902 44	− 470.512 353 263
0.097 173	0.000 496	− 510.853 10	− 511.614 366 288
0.097 173	0.002 77	− 507.963 51	− 511.529 123 768
0.097 173	0.016 5	− 492.307 44	− 511.527 340 862
0.097 173	0.031 1	− 476.010 65	− 511.425 063 578
0.097 173	0.079 0	− 388.309 91	− 504.260 615 827
0.097 173	0.117	− 330.502 45	− 503.099 515 758

[a] Molecular dynamics run mean potential.
[b] Potential minimum produced by mapping.

atom acting as a Lennard-Jones force center. They have evaluated the intermolecular part of the atom–atom pair correlation function for their model of liquid fluorine at the triple point [see their Figs. 9(a) and 10]. The qualitative resemblance to our result in Fig. 4 is reasonably close with corresponding peaks and valleys, though their short-range order is less distinct than ours. No doubt this reflects a real difference between the models in the respective short-distance forces between intact diatomic molecules. Unfortunately no diffraction experiments seem yet to have been performed on liquid fluorine to provide a measured g for comparison (though such results have been published for liquid Cl_2[27–28] and Br_2[28]).

IV. HIGH-TEMPERATURE DISSOCIATION

If the temperature is set sufficiently high, the vigorously vibrating fluorine molecules should begin to dissociate. At this stage the gap between the intramolecular and the intermolecular contribution to the pair correlation function (which is completely empty in Figs. 4, 5, and 8) will be invaded by pairs from both sides. We have carried out a series of high temperature molecular dynamics runs at two densities, the triple-point density already considered at lower T^* in the preceding Sec. III, and at one-eighth of the triple-point density, specifically

$$\rho^* = 0.012\ 147\,. \tag{4.1}$$

This lower density was achieved by doubling the dimensions of the cubical periodic cell, and it should be well below the critical density for fluorine (for most liquids the critical density is about 0.4 times the triple-point density[29]). The objective is to see how the dissociation equlibrium in the model depends both on T^* and on ρ^*.

We have employed a distance cutoff criterion in our calculations to identify chemical bonds, and by default to identify unbonded atoms produced by dissociation. Specifically we chose the following distance in the low-temperature pair correlation function gap:

$$r_c = 1.7\,. \tag{4.2}$$

Any atom pair closer than r_c was classified as chemically bonded. Unbonded atoms, of course, would have no neighbors closer than r_c and, hence, could be unambiguously counted in any instantaneous configuration adopted by the 1000-atom system.

The elementary definition of the fluorine atom association constant K_a is

$$K_a = c_2/(c_1)^2\,,$$
$$c_1 + \tfrac{1}{2}c_2 = \rho^*\,, \tag{4.3}$$

where c_1 and c_2 represent the reduced concentrations (number densities) of monomers and of diatomics, respectively. As a point of comparison for the molecular dynamics results it will be useful to have in hand an expression for the dilute-gas association constant. The classical statistical mechanical form is

$$K_a^{(0)}(T^*) = \left(\frac{2\pi}{\sigma^3}\right)\int_0^{r_c} \exp\left(\frac{-v_2(r)}{T^*}\right) r^2\,dr\,. \tag{4.4}$$

No solvation effects are present in $K_a^{(0)}$, so any systematic deviation from its predictions found in the molecular dynamics results should illuminate monomer and diatomic solvation at intermediate to high density. Table II shows some $K_a^{(0)}(T^*)$ values computed with the fluorine pair interaction (2.2), as well as the implied monomer fractions at the two ρ^* values used in the simulation.

Molecular dissociation begins to appear in the higher density simulation when the reduced temperature exceeds approximately 0.05. Figure 10 displays the pair correlation function for the state $T^* = 0.0790$ (1522 K), $\rho^* = 0.097\ 173$ (triple-point density). Filling of the gap between the intramolecular first peak and the intermolecular second peak is very clear. Figure 11 presents the pair correlation function at the same high density but with T^* increased to 0.117 (2254 K), with even greater peak broadening and gap filling.

Figures 12 and 13 show pair correlation functions for two equilibrated high temperature states at the lower density $\rho^* = 0.012\ 147$. The intermolecular portions are quite featureless by contrast with the higher density cases, Figs. 10

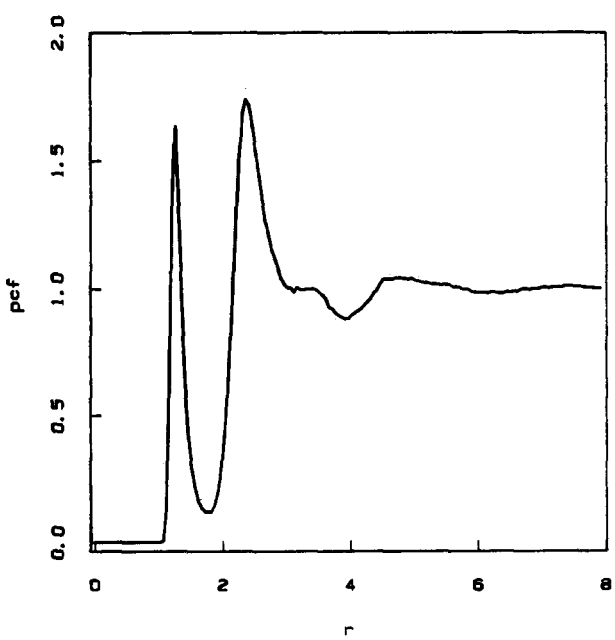

FIG. 10. Pair correlation function for the partially dissociated state at $T^* = 0.0790$, $\rho^* = 0.097\ 173$.

TABLE II. Gas-phase association constant and implied monomer fractions based on the model fluorine pair interaction.

T^*	$K_a^{(0)}(T^*)$[a]	c_1/ρ^* ($\rho^* = 0.012\,147$)	c_1/ρ^* ($\rho^* = 0.097\,173$)
0.02	3.3062×10^{21}	2.2316×10^{-10}	7.8900×10^{-11}
0.03	2.3686×10^{14}	8.3375×10^{-7}	2.9478×10^{-7}
0.04	6.6589×10^{10}	4.9724×10^{-5}	1.7581×10^{-5}
0.05	5.0838×10^{8}	5.6894×10^{-4}	2.0119×10^{-4}
0.06	2.0147×10^{7}	2.8547×10^{-3}	1.0102×10^{-3}
0.07	2.0416×10^{6}	8.9402×10^{-3}	3.1701×10^{-3}
0.08	3.7156×10^{5}	2.0830×10^{-2}	7.4150×10^{-3}
0.09	9.9819×10^{4}	3.9797×10^{-2}	1.4257×10^{-2}
0.10	3.5193×10^{4}	6.6100×10^{-2}	2.3893×10^{-2}
0.11	1.5111×10^{4}	9.9078×10^{-2}	3.6231×10^{-2}
0.12	7.5181×10^{3}	1.3744×10^{-1}	5.0972×10^{-2}
0.13	4.1870×10^{3}	1.7961×10^{-1}	6.7697×10^{-2}
0.14	2.5468×10^{3}	2.2398×10^{-1}	8.5947×10^{-2}
0.15	1.6617×10^{3}	2.6911×10^{-1}	1.0527×10^{-1}
0.20	3.8619×10^{2}	4.7369×10^{-1}	2.0574×10^{-1}
0.25	1.6631×10^{2}	6.1632×10^{-1}	2.9531×10^{-1}
0.30	9.6498×10^{1}	7.0703×10^{-1}	3.6734×10^{-1}
0.35	6.6048×10^{1}	7.6515×10^{-1}	4.2376×10^{-1}
0.40	4.9991×10^{1}	8.0382×10^{-1}	4.6800×10^{-1}
0.45	4.0403×10^{1}	8.3068×10^{-1}	5.0311×10^{-1}
0.50	3.4159×10^{1}	8.5008×10^{-1}	5.3176×10^{-1}

[a] Dimensionless association constant defined in Eq. (4.4), with $r_c = 1.7$.

and 11. Nevertheless, pairs are again in transit across the gap region.

Table III shows some results for the mean numbers of monomers and reveals a subtlety of interpretation. The cutoff definition of chemical bonding leads to a curious ambiguity. Occasionally we find transitory fluorine trimers owing to the violent vibrations and collisions underway at high temperature. This can produce unstable groupings of three atoms with one atom simultaneously closer than r_c to two others. Even transient linear tetramers of this sort have infrequently been detected. On chemical grounds it seems reasonable to regard the trimers as a monomer momentarily closely solvated by a dimer. The notation "$n + m$" in Table III indicates the presence of n unambiguous monomers and m present as parts of trimers. In any case the mean number of monomers is far larger at both densities than would be inferred from the dilute gas $K_a^{(0)}$ values in Table II. Evidently the solvation of monomers provides a driving force for enhanced dissociation.

Table III shows that under essentially constant temperature conditions reducing the system density by a factor of 8 causes the degree of dissociation to decline substantially. This violates naive expectation based on Le Chatelier's prin-

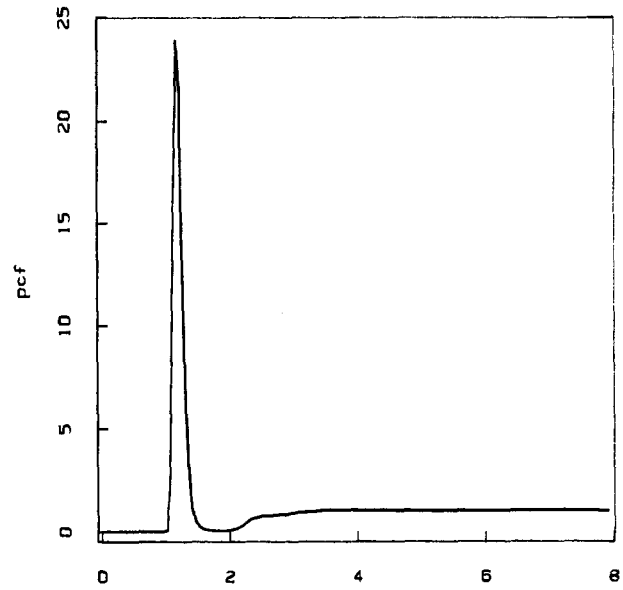

FIG. 12. Pair correlation function for the partially dissociated state at $T^* = 0.0796$, $\rho^* = 0.012\,147$.

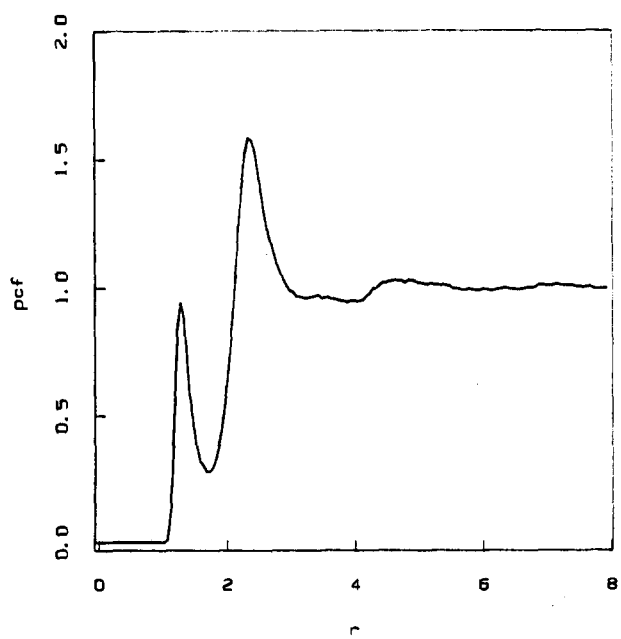

FIG. 11. Pair correlation function for the partially dissociated state at $T^* = 0.117$, $\rho^* = 0.097\,173$.

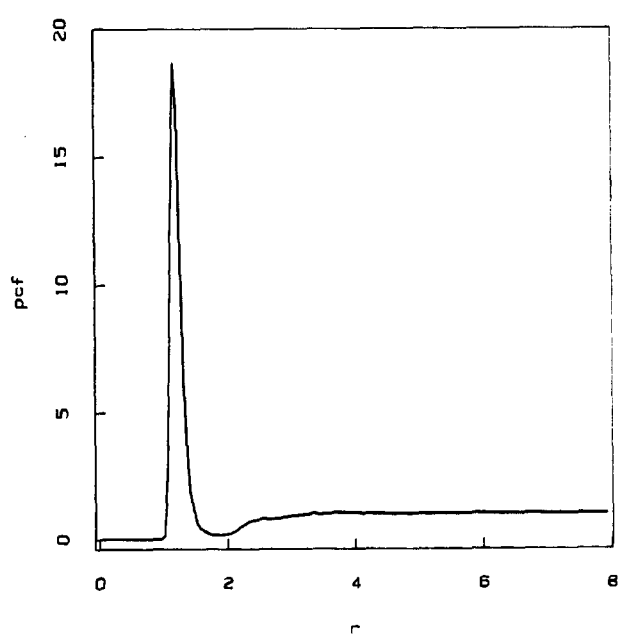

FIG. 13. Pair correlation function for the partially dissociated state at $T^* = 0.124$, $\rho^* = 0.012\,147$.

TABLE III. Numbers of fluorine atoms produced by dissociation at high temperature.

T^*	ρ^*	Monomer number[a,b]	Quenched monomer number[c]
0.0790	0.097 173	173 + 3	42
0.117	0.097 173	274 + 12	48
0.0796	0.012 147	44	42
0.124	0.012 147	117 + 1	84

[a] Numbers refer to the final configurations of the respective molecular dynamics runs.
[b] The notation $n + m$ denotes n unbonded F atoms and m linear F_3 units.
[c] Numbers refer to the potential energy minimum obtained from the final molecular dynamics configuration by steepest-descent mapping.

ciple which would hold that increasing the volume should favor unbonded species.[30] Evidently the effect of solvation is sufficiently sensitive to density to overturn that expectation.

Steepest-descent mapping can be applied to configurations in states with dissociation. Not only is the image of short-range order enhanced as before, but bonding ambiguities as presented by linear trimers, etc., are entirely removed.[31] Figures 14–17, respectively, display the quenched pair correlation functions obtained from final configurations for the runs of Figs. 10–13. The mapping in each case has totally restored the gap between intramolecular and intermolecular pairs. Furthermore, all atoms after mapping have either one or no bonds by the cutoff definition, corresponding unambiguously to diatomic and to monatomic species.

The last column in Table III demonstrates that the structural clarity induced by steepest-descent mapping has been bought at a significant price. The number of monomers has declined substantially. Evidently many atoms identified as "unbonded" in a chemically conventional way in high-temperature states are still within a weak attractive neighborhood of another such atom; the steepest-descent procedure then manages to bring them back together. The last column in Table III can be interpreted as giving an "inherent" extent of dissociation arising from pure packing considerations, which anharmonic thermal vibrations then augment to yield the conventional observed extent of dissociation.

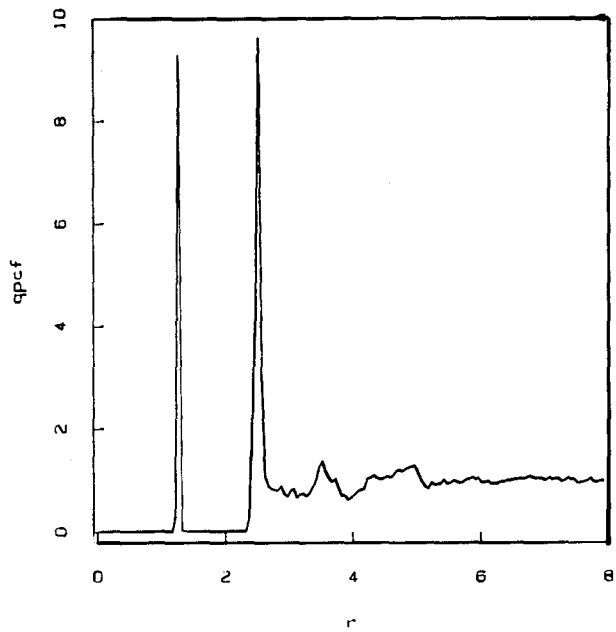

FIG. 15. Quenched pair correlation function from the partially dissociated state at $T^* = 0.117, \rho^* = 0.097\,173$.

The presence of inherently dissociated atoms in quenches from high-temperature causes the quench pair correlation functions to differ characteristically from those giving the inherent structure of the low-temperature undissociated liquid. First, the intramolecular peak encompasses less area corresponding to the fewer bonds present. Second,

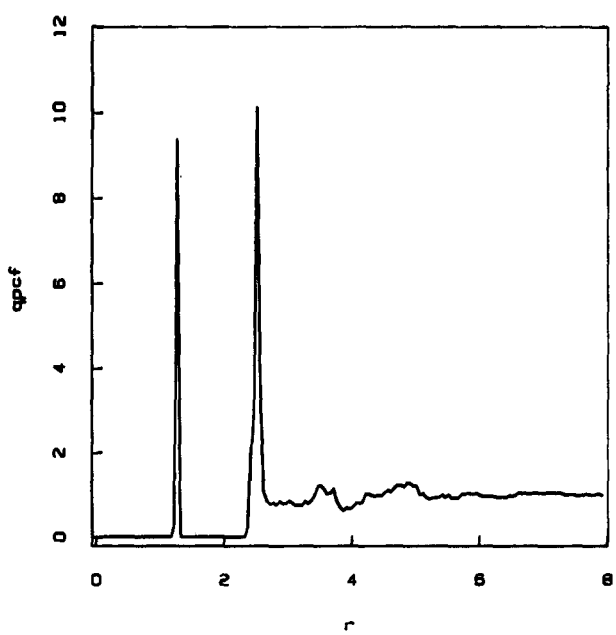

FIG. 14. Quenched pair correlation function from the partially dissociated state $T^* = 0.0790, \rho^* = 0.097\,173$.

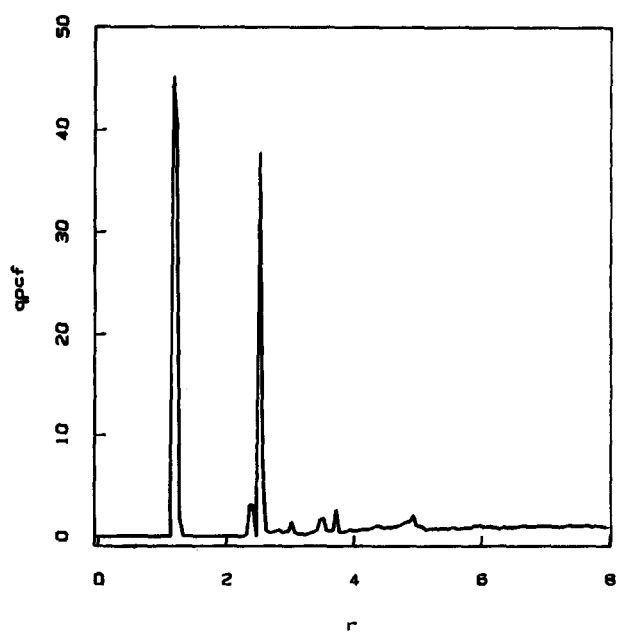

FIG. 16. Quenched pair correlation function from the partially dissociated state at $T^* = 0.0796, \rho^* = 0.012\,147$.

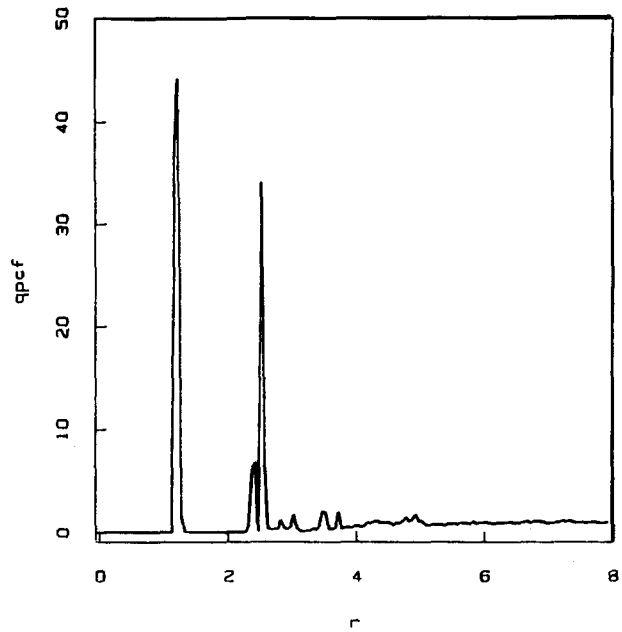

FIG. 17. Quenched pair correlation function from the partially dissociated state at $T^* = 0.124$, $\rho^* = 0.012\,147$.

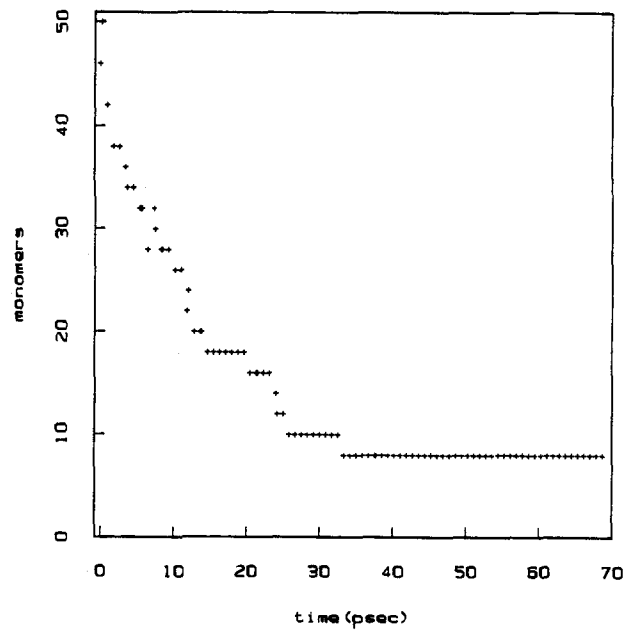

FIG. 18. Number of unbonded fluorine atoms vs time. The system was prepared in a partially dissociated state at $T^* = 0.080$, then thermostated at the lower temperature $T^* = 0.019$ at $t = 0$.

monomeric atoms interact more strongly with, and tend to be closer to, a neighboring diatomic than would atoms in another diatomic. Consequently, we see that the first intermolecular peak of the quench pair correlation function broadens a bit in the high density case (Figs. 14 and 15) and splits into an asymmetric doublet in the low density case (Figs. 16 and 17).

In principle, the molecular dynamics simulation technique with models of the type considered here can be a powerful tool to study chemical kinetics. Separate rate constants k_a and k_d for association–dissociation reactions of the general type

$$\mathrm{XY} \underset{k_a}{\overset{k_d}{\rightleftarrows}} \mathrm{X} + \mathrm{Y} \tag{4.5}$$

could be extracted from molecular dynamics data concerning (a) the equilibrium constant for the given temperature and density of interest, and (b) the time-dependent autocorrelation function of the extent of reaction in the same thermodynamic state. Of course, molecular dynamics is capable of probing chemical relaxation from initial states far from equilibrium, and is not limited to the linear response regime.

Figure 18 shows an example of chemical relaxation in the lower density case, $\rho^* = 0.012\,47$. The 1000-atom system was prepared in a partially dissociated state at $T^* \cong 0.080$, then rapidly cooled to (and thermostated at) $T^* \cong 0.019$. At this latter temperature the concentration of monomeric atoms at equilibrium is expected to be vanishingly small so recombination occurs. Figure 18 shows how the number of those monomers declines during a reaction time of 1644τ (68.75 ps). At the final stage eight widely separated monomers remained whose eventual recombination would be determined by slow diffusion in the large system volume. Available computer resources did not allow us to run the reaction to completion, but the trend seems clear.

V. VAPOR CONDENSATION

A lengthy molecular dynamics sequence was generated at the lower density $\rho^* = 0.012\,47$ in order to see if the model fluorine system initially in the vapor phase could be observed spontaneously to condense into a liquid as the temperature declined. This would have the benefit of checking on the higher density used and the short-range order found earlier for the low-temperature liquid. For this purpose the system was initialized as undissociated diatomics, carefully equilibrated at $T^* = 0.0195$, and observed to remain totally undissociated at this temperature for 400τ (16.7 ps). The

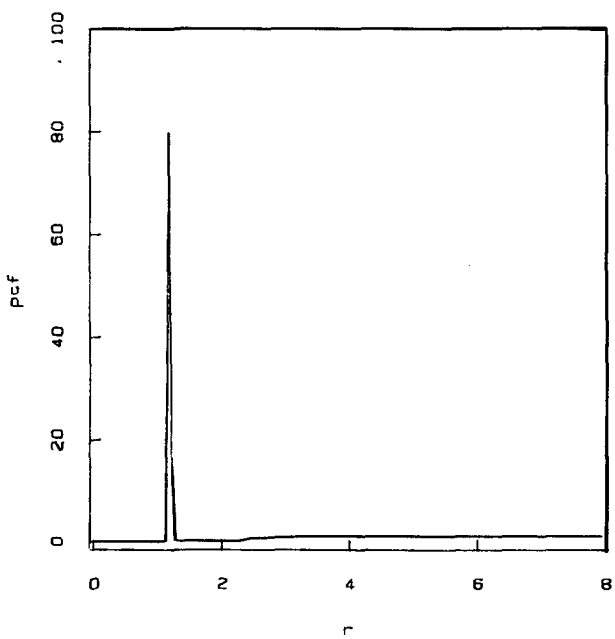

FIG. 19. Pair correlation function for the fully associated compressed gas at $T^* = 0.0195$, $\rho^* = 0.012\,147$.

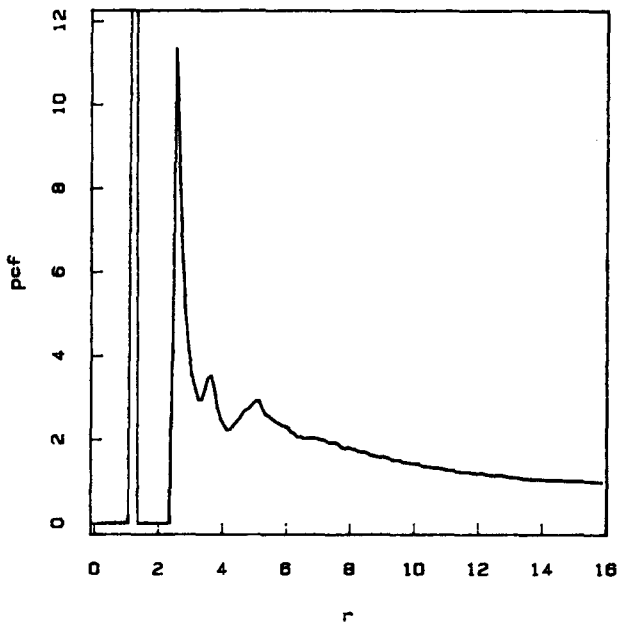

FIG. 20. Pair correlation function in the condensed and inhomogeneous state at $T^* = 0.001\,23, \rho^* = 0.012\,147$.

system subsequently was cooled in stages, each with a small temperature reduction and at least partial reequilibration, during a total time span of $11\,232\tau$ (469.7 ps).

At the beginning of the cooling process the intermolecular part of the pair correlation function, shown in Fig. 19, is virtually featureless (except for the influence of overlap exclusions). This is just what should be expected for a homogeneous gas. But after sufficient cooling it becomes obvious that the model spontaneously forms a denser aggregate in part of the cubical box, leaving empty space behind. Figure 20 provides the pair correlation function at the much lower temperature $T^* = 0.001\,23$, with strongly enhanced local correlation slowly tailing off to subrandom values at large distance ($g < 1$), just as expected when aggregation is present.

That aggregation has been induced by cooling is clearly confirmed in Fig. 21. This gives a view of the collection of 500 diatomics in the cubic periodicity cell at the end of the molecular dynamics cooling sequence. The spatial inhomogeneity of the matter distribution is obvious.

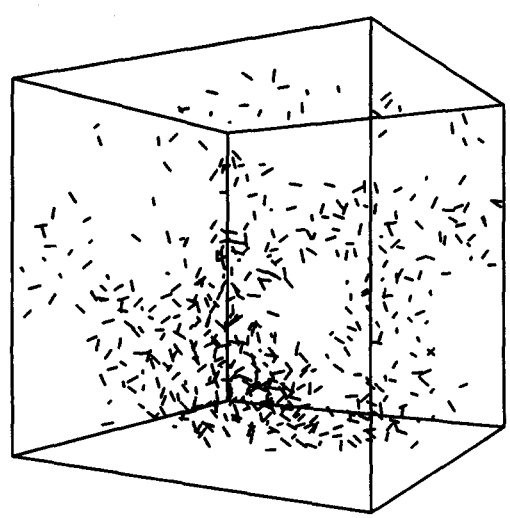

FIG. 21. System final configuration from the condensed and inhomogeneous state of Fig. 20.

VI. CONCLUDING REMARKS

The present paper provides an approximate model for the highly reactive element fluorine. Utilizing the molecular dynamics simulation method with systems of 1000 atoms we have verified at least qualitatively that this model possesses the major physical and chemical properties required. In particular, we were able to examine the nature of short-range order in the liquid, and to observe the dissociation equilibrium that yields monomeric fluorine from diatomic molecules at high temperature.

A basic assumption in our model is that the many-atom potential energy function Φ comprises only two-atom and three-atom contributions. In fact, our specific choices for these component functions v_2 and v_3 may not be close to optimal. As more experimental and theoretical data on the properties of fluorine in bulk and in clusters of molecules emerge it should be clear how to refine the v_2 and v_3 functions. It should easily be possible, e.g., to soften repulsive interactions between close pairs of diatomics and to increase the magnitude of van der Waals attractions.

Classical statistical mechanics has been used throughout this paper. Because fluorine atoms are light, however, quantum corrections are likely to be significant particularly at low temperatures. The currently popular path integral techniques that have been applied to simulations of other light-particle systems[32] could easily be adapted to our fluorine model.

The heavy halogen iodine has been observed to transform under increasing pressure from a molecular crystal with identifiable I_2 units to a monatomic metallic state.[33] It seems sensible to suppose that the other halogens, specifically fluorine, would display analogous behavior. On the basis of what has been learned in the present project it is reasonable to conclude that high-pressure simulations with our fluorine model would be a helpful tool to study this transformation. High-pressure shifts the balance between v_2 and v_3 contributions, making it geometrically less favorable for univalent bonding. Simulation should be capable of estimating the transition pressure in fluorine and the discontinuities at that transition in thermodynamic and crystallographic properties.

[1] J. P. Hansen and I. R. McDonald, *Theory of Simple Liquids* (Academic, New York, 1976), Chap. 3.
[2] *Molecular Dynamics Simulation of Statistical Mechanical Systems*, edited by G. Ciccoti and W. G. Hoover (North-Holland, Amsterdam, 1987).
[3] S. F. Trevino and D. H. Tsai, J. Chem. Phys. **81**, 248 (1984).
[4] D. L. Bunker and B. S. Jacobson, J. Am. Chem. Soc. **94**, 1843 (1972).
[5] A. J. Stace and J. N. Murrell, Mol. Phys. **33**, 1 (1977).
[6] F. H. Stillinger, Physica A **140**, 142 (1986).
[7] F. H. Stillinger and T. A. Weber, Phys. Rev. B **31**, 5262 (1985); **33**, 1451(E) (1986).
[8] F. F. Abraham and J. Broughton, Phys. Rev. Lett. **56**, 734 (1986).

[9]M. D. Kluge, J. R. Ray, and A. Rahman, J. Chem. Phys. **87**, 2336 (1987).
[10]F. H. Stillinger, T. A. Weber, and R. A. LaViolette, J. Chem. Phys. **85**, 6460 (1986).
[11]F. H. Stillinger and T. A. Weber, J. Phys. Chem. **91**, 4899 (1987).
[12]K. Singer, A. Taylor, and J. V. L. Singer, Mol. Phys. **33**, 1757 (1977).
[13]G. Herzberg, *Molecular Spectra and Molecular Structure. I. Spectra of Diatomic Molecules* (Van Nostrand Reinhold, New York, 1950), p. 527.
[14]K. P. Huber and G. Herzberg, *Molecular Spectra and Molecular Structure. IV. Constants of Diatomic Molecules* (Van Nostrand Reinhold, New York, 1979), p. 214.
[15]P. Siegbahn and B. Liu, J. Chem. Phys. **68**, 2457 (1978).
[16]J. P. Bergsma, J. R. Reimers, K. R. Wilson, and J. T. Hynes, J. Chem. Phys. **85**, 5625 (1986).
[17]D. J. Hankinson and T. A. Weber (to be published).
[18]J. Donohue, *The Structures of the Elements* (Krieger, Malabar, FL, 1982), p. 394.
[19]*Gmelins Handbuch der Anorganischen Chemie. Fluor*, Supplementary Vol. 5 (Chemie, Weinheim, 1959), p. 87.
[20]C. W. Gear, *Numerical Initial-Value Problems in Ordinary Differential Equations* (Prentice-Hall, Englewood Cliffs, 1971).
[21]F. H. Stillinger and T. A. Weber, Phys. Rev. A **25**, 978 (1982).
[22]F. H. Stillinger and T. A. Weber, Phys. Rev. A **28**, 2408 (1983).
[23]F. H. Stillinger and T. A. Weber, J. Chem. Phys. **80**, 4434 (1984).
[24]T. A. Weber and F. H. Stillinger, Phys. Rev. B **32**, 5402 (1985).
[25]F. H. Stillinger and R. A. LaViolette, Phys. Rev. B **34**, 5136 (1986).
[26]F. H. Stillinger and T. A. Weber, Science **225**, 983 (1984).
[27]J. D. Sullivan and P. A. Egelstaff, Chem. Phys. **89**, 167 (1984).
[28]P. Bisanti and F. Sacchetti, Mol. Phys. **54**, 255 (1985).
[29]E. A. Guggenheim, *Thermodynamics* (North-Holland, Amsterdam, 1950), pp. 140-141.
[30]G. G. Hawley, *The Condensed Chemical Dictionary*, 10th ed. (Van Nostrand Reinhold, New York, 1981), p. 611.
[31]T. A. Weber and F. H. Stillinger, J. Chem. Phys. **87**, 3252 (1987).
[32]R. A. Kuharski and P. J. Rossky, J. Chem. Phys. **82**, 5164 (1985).
[33]Y. Fujii, K. Hase, N. Hamaya, Y. Ohishi, A. Onodera, O. Shimomura, and K. Takemura, Phys. Rev. Lett. **58**, 796 (1987).